BeamDocs 3335

Analysis of beam-based measurement of absolute phase jitter between an accelerating structure and a relativistic electron bunch

P. Piot*

Northern Illinois University, DeKalb IL 60115, USA and

Fermi National Accelerator Laboratory, Batavia, IL 60510, USA

(Dated: March 21, 2008)

We describe and analyze a beam-based technique for precisely measuring the absolute phase jitter between the electromagnetic field established in an accelerating module and a relativistic electron bunch being accelerated by this module. The performance of the proposed beam-based method is numerically explored using, as an example, the International Linear Collider (ILC) test accelerator currently in construction at Fermilab.

I. INTRODUCTION

The International Linear Collider (ILC) along with several on-going or proposed accelerator-based light sources incorporate superconducting accelerating structures with unprecedented requirements on time and energy stability. For instance, the currently envisioned ILC bunch compression system, downstream of the electron and positron damping rings, calls for an absolute root mean square (rms) phase jitter between the beam and the cavity's electromagnetic field of less than 0.25° (at 1.3 GHz, or less than 150 fs), while the specified maximum relative field amplitude jitter should be 0.07% [1]. Several facilities worldwide are being constructed and/or operated to develop and characterize low level radio-frequency control systems capable of meeting the aforementioned specifications [3]. Measuring such a jitter is a challenging task especially when accounting for other possible sources of jitter upstream of the system to be characterized. The transient beam loading method can provide a rough estimate of the phase between the beam and the cavity's field (with 1° accuracy) but requires high charge bunches [2]. In this Note we explore a technique that can be used to measure the phase jitter while operating the accelerator with nominal conditions (beam structure charge and set-point of the accelerating module).

*Work supported by Northern Illinois University under DE-FG02-06ER41435 with U.S. DOE and by the Fermi Research Alliance LLC under DE-AC02-07CH11359 with U.S. DOE.; Electronic address: piot@nicadd.niu.edu

We first detail the proposed procedure and develop a one-dimensional model of the longitudinal beam dynamics to quickly estimate the impact of various sources of jitter in the beam-line downstream of the to-be-tested accelerating module. We investigate the practical implementation of the method and its performances using, as an example, the ILC test accelerator (ILCTA) currently in construction at Fermilab [4]. We also address possible limitations coming from other sources of jitter (e.g. charge jitter, long range wakefields) and finally consider instrumental errors.

II. PROPOSED TECHNIQUE

We consider the problem of measuring the phase jitter between an electron bunch and the electric field established in an accelerating structure. We assume an accelerating structure to be characterized by the normalized peak energy gain $\Gamma \equiv \frac{eV}{m_e c^2}$ it can provide to the bunch and the phase between the accelerating field and the bunch Φ. With such a simple model the final Lorentz factor γ_k of a bunch k, with initial Lorentz factor $\gamma_{0,k}$ and arrival time t_k at the accelerating module entrance, is [15],

$$\gamma_k = \gamma_{0,k} + \Gamma_k \cos(\Phi_k), \tag{1}$$

where $\Gamma_k \equiv \Gamma + \delta\gamma_k$ is the peak normalized energy gain seen by bunch k and $\delta\gamma_k$ the fluctuation in field amplitude compared to the average value $\bar{\gamma}$ with its ensemble averaging $\langle \delta\gamma_k \rangle = 0$. Similarly $\Phi_k \equiv \omega(t_k - \bar{t}) + \Phi + \delta\phi_k$ is the phase between the field and the bunch k, Φ is the set phase, $\delta\phi_k$ is the phase error arising from rf-system fluctuation as bunch k is being accelerated, and $\omega\delta t_k$ (where $\delta t_k \equiv t_k - \bar{t}$) represents the contribution to phase error arising from an injection timing error. In principle, the following parameters can be measured: δt_k, Φ with respect to the master oscillator and the accelerating voltage Γ.

A bunch with time-of-arrival $t_{0,k}$ at the entrance of the accelerating module will have a final time-of-arrival t_k, downstream of the accelerating module, given by

$$t_k = t_{0,k} + \left(1 + \frac{L}{\gamma_k \gamma_{0,k}}\right), \tag{2}$$

where L is the effective accelerating length. For the case of relativistic incoming bunch ($\gamma_k, \gamma_{0,k} \to \infty$), $t_k \simeq t_{0,k} + L/c$ and the final time-of-arrival does not contain information on the accelerating module phase or amplitude jitter. Thus an accurate measurement of the phase between the bunch

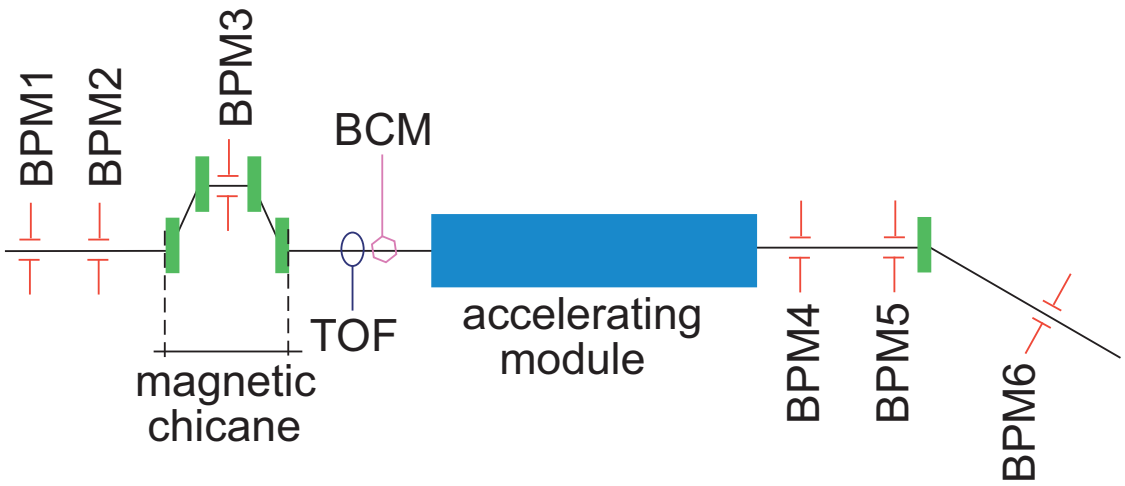

FIG. 1: Overview of the generic system assumed in this paper. The "accelerating module" is flanked between a magnetic chicane and a spectrometer (both can be used to measure the energy of the bunch prior and after the module). A time-of-flight monitor (TOF) can be used to measure the timing of an electron bunch, BPM refers to beam position monitors and BCM stands for beam current monitor.

and electromagnetic field requires an energy measurement.

Given the measured energy, γ_k, of a bunch downstream of the accelerating module, the normalized accelerating voltage amplitude, Γ_k, the relative time-of-arrival δt_k, and the measured set phase Φ, we formally retrieve the phase offset of the bunch k with respect to the field in the cavity via

$$\underline{\delta\phi_k} \equiv -\omega\delta t_k - \Phi + \arccos\left(\frac{\gamma_k - \gamma_{0,k}}{\Gamma_k}\right). \tag{3}$$

Practically, uncertainties on the energy measurements might result in $\frac{\gamma_k-\gamma_{0,k}}{\Gamma_k} > 1$, especially for on-crest operation, which would result in complex value of the $\delta\phi_k$, such an nonphysical value is henceforth disregarded. We also note that it might not be generally possible to measure Γ_k for each bunch especially when considering consecutive bunches in a high average current linac. We therefore define the "gradient-averaged" quantity

$$\underline{\underline{\delta\phi_k}} \equiv -\omega\delta t_k - \Phi + \arccos\left(\frac{\gamma_k - \gamma_{0,k}}{\Gamma}\right), \tag{4}$$

where Γ represents the value of Γ_k averaged over several bunches. Finally we note that an alternative way of retrieving $\delta\phi_k$ consists in considering the quantity

$$\widetilde{\gamma_{0,k}} \;=\; \gamma_k - \Gamma_k\cos(\omega\delta t_k + \Phi)$$

where the quantities on the right-hand-side are all measured. Expliciting γ_k gives

$$\begin{aligned}\widetilde{\gamma_{0,k}} &= \gamma_{0,k} + \Gamma_k \left[\cos(\omega\delta t_k + \Phi + \delta\phi_k) - \cos(\omega\delta t_k + \Phi)\right], \\ &\overset{\delta\phi_k \ll 1}{\rightarrow} \gamma_{0,k} - \Gamma_k \delta\phi_k \sin(\omega\delta t_k + \Phi),\end{aligned} \tag{5}$$

where a first order Taylor expansion in $\delta\phi_k$ was used. For each bunch, using Equations 5 and 6, we can compute the phase offset $\delta\phi_k$ via:

$$\overline{\delta\phi_k} \equiv \frac{-\gamma_k + \Gamma_k \cos(\omega\delta t_k + \Phi) + \gamma_{0,k}}{\Gamma_k \sin(\omega\delta t_k + \Phi)}, \tag{6}$$

and we can also defined the corresponding "gradient-averaged" quantity as

$$\overline{\overline{\delta\phi_k}} \equiv \frac{-\gamma_k + \Gamma \cos(\omega\delta t_k + \Phi) + \gamma_{0,k}}{\Gamma \sin(\omega\delta t_k + \Phi)}. \tag{7}$$

The advantage of the Taylor expansion lies in the absence of inverse trigonometric function. Ideally a measurement of the phase jitter requires a measurement of $\gamma_{0,k}$ and γ_k the energies of the bunch upstream and downstream of the cryomodule, δt_k relative time-of-flight of the bunch (can be measured upstream or downstream of the cryomodule), Φ the average set phase of the cryomodule, and Γ_k the amplitude of the accelerating voltage in the cryomodule.

Because a measurement of the phase jitter only involves measurements of the first order moments we ignore single bunch dynamics and consider each bunch to be point-like macroparticle. Ensemble averaging a series of phase offsets measured for several bunches provide the rms phase jitter $\sigma_\phi \equiv \langle \delta\phi_k^2 \rangle^{1/2}$. To the four values of $\delta\phi_k$ defined above (in Eq. 3, 4, 6, and 7), we respectively associate the rms values $\underline{\sigma}_\phi$, $\underline{\underline{\sigma}}_\phi$, $\overline{\sigma}_\phi$, and $\overline{\overline{\sigma}}_\phi$.

III. INFLUENCE OF UPSTREAM JITTER SOURCES

A high-precision measurement of the phase jitter needs to account and disentangle the other sources of possible jitter. We now considered the accelerator beaming upstream of the accelerating module to be characterized – henceforth referred to as "injector". An injector consists of an electron source and a booster section. We previously hinted that a measurement of the energy of the bunch prior to entering the accelerating module might be needed. Measuring the beam's energy

does not a fortiori require a dispersive section: intercepting diagnostics such as interferometric transition radiation technique can be used [5]. We however anticipate the use of a dispersive bump that includes an electromagnetic beam position monitor located at a high dispersion point would provide a precise, simple, and non-intercepting way of measuring the beam's energy upstream of the accelerating module. Such a dispersive bump, also referred to as magnetic chicane, has other benefits: it can also be used to compress the bunch, e.g. to possibly probe the longitudinal wake potential of the accelerating structure [7]. A magnetic chicane introduces an energy-dependent path-length which results in the final time-of-arrival

$$t_k \;=\; t_{k,0} + \frac{R_{56}}{c}\frac{\gamma - \gamma_{ref}}{\gamma_{ref}}, \tag{8}$$

where $t_{k,0}$ refers to the time-of-arrival at the chicane's entrance, γ_{ref} is the reference Lorentz factor for which the chicane is setup, and R_{56} is the longitudinal dispersion associated to the chicane. Therefore the chicane couples an incoming energy jitter to a time jitter because of the chicane. Thus it is arguable that the magnetic chicane might introduce an intolerable time jitter which will prevent a precise measurement of the beam/accelerating module phase jitter.

We now on specialize to the photoinjector option for the ILCTA injector. The electron source is based on a 1+1/2 cell rf cavity (henceforth refer to as rf gun) operating on the $\mathrm{TM}_{010,\pi}$ mode. An ultraviolet (uv) laser pulse impinges a high quantum efficiency Cesium-Telluride photo-cathode located on the back plate of the rf-gun. The photoemitted high charge electron bunch has an energy of $\sim$ 4 MeV upon exit from the rf-gun. The bunch is then further accelerated by two booster cavities to a final maximum energy of approximately 40 to 50 MeV depending on the accelerating structure phases. Besides standards optical element the injector beamline, before injecting the beam in the accelerating module(s), incorporates a magnetic chicane with longitudinal dispersion $R_{56} \simeq -20$ cm. In Figure 2 we show the time and fractional energy jitter upstream of the accelerating module for different plausible phase and amplitude rms jitter associated to the component listed in Table I. For these calculations we assumed all the components phase and amplitude to have the same rms jitter values.

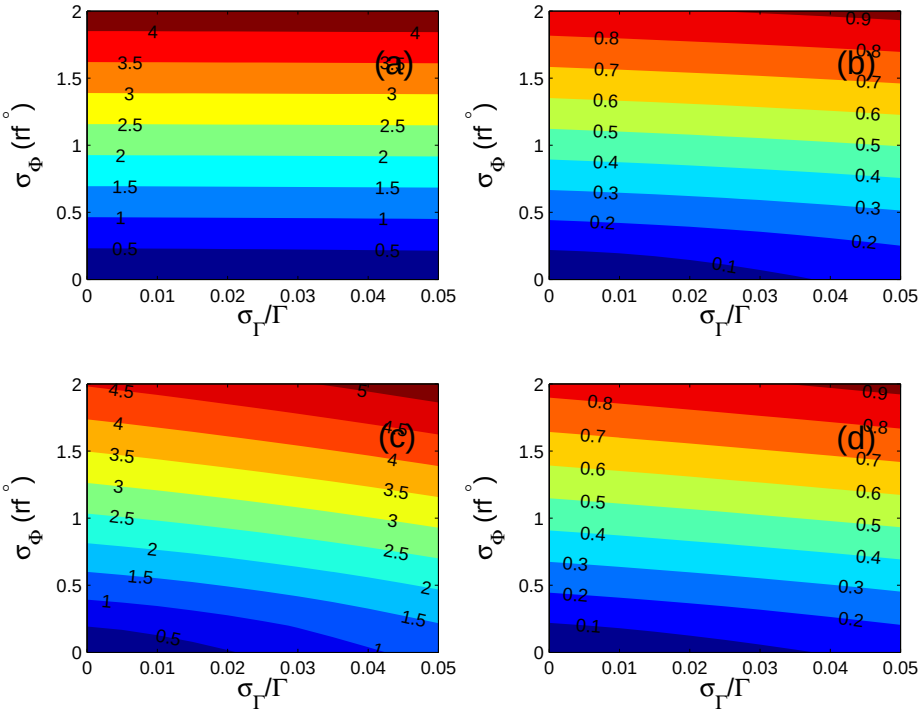

FIG. 2: Root mean square (rms) time [(a) and (c)] and Lorentz factor [(c) and (d)] jitters at the the accelerating structure entrance as a function of the assumed rms jitter for the phase and amplitude associated to the injector components. The cases of compressor turned off [(a) and (b)] and on [(c) and (d)] are considered. The numbers associated to isocontours in the left column correspond to the rms time jitter in picoseconds while those in the right column corresponds to the Lorentz factor jitter and are unit-less. The same seed for the random number generator was used for all the simulations shown here.

IV. NUMERICAL SIMULATION OF PHASE JITTER MEASUREMENTS

A one-dimensional model of the longitudinal beam dynamics was developed to quickly estimate the impact of various sources of jitter. The program is based on MATLAB [8]. The implementation of each element is described in the Appendix. The program tracks a series of bunch represented by macroparticles in the longitudinal phase space (t, γ). The first macroparticle experience the ideal, jitter free, electric fields while the subsequent ones macroparticles are subject to non ideal fields due to amplitude and phase jitters. We consider all the phase and amplitude jitters to follow a Gaussian probability function sand take the ILCTA photoinjector configuration with main parameters affecting the longitudinal beam dynamics listed in Table I. For the sake of simplicity we consider all the phase and amplitude jitters associated to the photoinjector components to be distributed with respective rms values of 2 deg and 1 %.

The accelerating module considered is a standard eight-cavities TESLA type cryomodule. Sim-

parameter	value	units
laser launch phase	40	deg
rf gun peak E-field	39	MV/m
cavity 1 peak E-field	25	MV/m
cavity 1 off-crest phase	0	deg
cavity 2 peak E-field	50	MV/m
cavity 2 off-crest phase	0	deg

TABLE I: Proposed parameters for the ILCTA photoinjector option.

ulations of phase jitter measurement were performed for various operating conditions of the accelerating cryomodule. For all cases reported below, the cryomodule maximum energy gain was 200 MeV, a value consistent with 8 cavities operated to provide a 25 MeV energy gain. We assumed the field amplitude jitter in the cryomodule to be 1 % and the phase jitter between the module field and bunch to be 0.05 deg – a factor 5 below the specified value for the ILC bunch compressor system [1]. The operating phase of the accelerating module was varied and for each set point ten randomly independent series of fifty bunches were tracked through the injector and module thereby experiencing randomly distributed phase and amplitude jitters. The four methods discussed in Section 2 were implemented to retrieve the "measured" phase jitters. We also considered both cases when the magnetic chicane located upstream of the accelerating module (see Fig. 1) is turned on and off (when on, the chicane enables an energy measurement upstream of the accelerating module). The results are gathered in Figures 3 and 4 respectively associated to the two cases of magnetic chicane settings.

The simulations support the use Equations 6 and 7 to retrieve the phase jitter instead of Equations 3 and 4. A comparison of the bottom rows of Figures 3 and 4 shows that results obtained when the magnetic chicane is turned on, and the energy upstream of the cryomodule measured, are more precise over a larger ranges of operating phases. Such a trend is confirmed in Figure 5 where, for four cases of cryomodule operating phases, the fractional field amplitude jitter was varied and the measured phase jitter was computed for the the cases of chicane on and off. For the calculations reported in Figure 5, the "measured" rms jitter, σ_ϕ, was obtained using Equation 6.

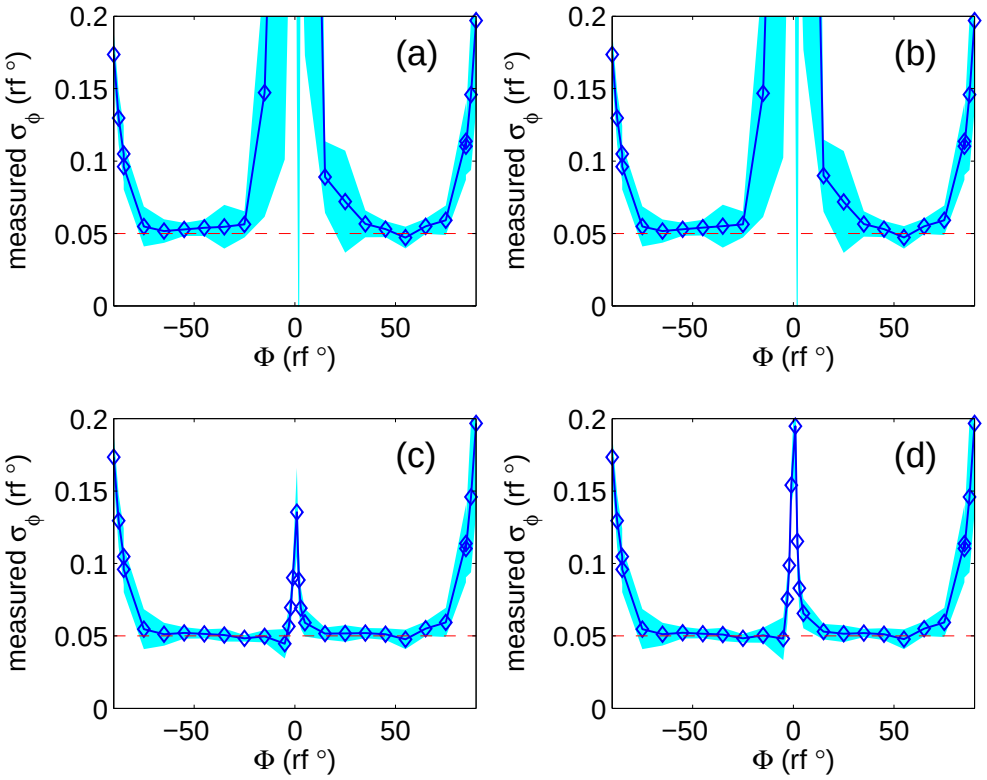

FIG. 3: Retrieved phase jitter when the magnetic chicane is turned on and for an accelerating module rms fractional jitter of 10^{-2}. Plots (a), (b), (c), and (d) respectively correspond to measured rms phase jitter based on Equations 3, 4, 6, and 7.

V. OTHER SOURCES OF JITTER

A. Bunch-to-bunch charge fluctuation

To date we have considered time and energy jitters associated to a bunch that are imparted by external fields. We now consider possible jitter resulting from the bunch self fields. A high charge (several nC) electron bunch has its dynamics significantly impacted by collective effects such as space charge and radiative effects. Collective effects depend on the bunch charge which, over short time scale (comparable to the duration of few rf macropulses) is mainly given by the photocathode drive laser intensity. If all the bunched had the same charge, the analysis performed in the previous section would hold even when considering energy losses due to collective effect: the variance of the measured fractional energy would still be representative of the rms phase jitter – formally we would have the measured energy to be off the form $X = A + Y$ with $\langle Y \rangle = 0$ and A being a constant offset therefore we would have in term of variances $\langle X^2 \rangle = \langle Y^2 \rangle$.

If the charge varies from bunch to bunch, collective effects might changes the bunch properties

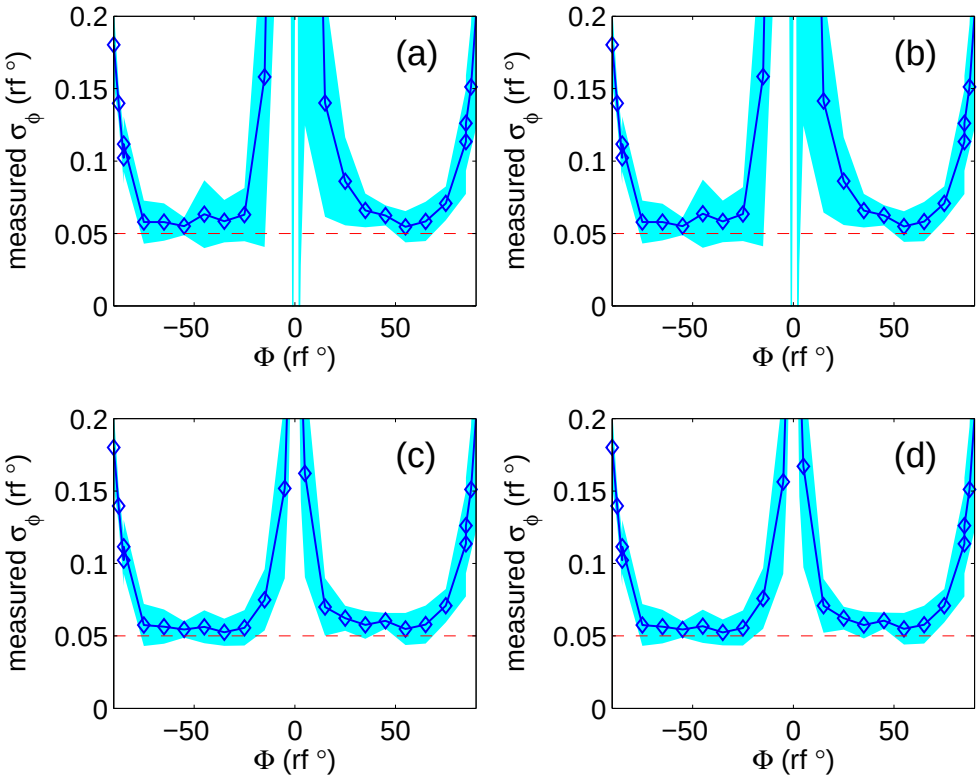

FIG. 4: Retrieved phase jitter when the magnetic chicane is turned off and for an accelerating module rms fractional jitter of 10^{-2}. Plots (a), (b), (c), and (d) respectively correspond to measured rms phase jitter based on Equations 3, 4, 6, and 7.

thereby complicating the phase jitter measurement. Among the various collective effects, we first note that the longitudinal space charge force results in an energy spread dilution that does not affect the first order moments of the bunch (i.e. the bunch does not lose or gain energy). The two main direct sources of charge-induced jitters come from radiative effects: coherent synchrotron radiation (CSR) and wakefield. If the bunch energy is measured upstream of the accelerating module the effect of these radiative effects will be included in the incoming jitter measurement up to the magnetic chicane midpoint. Only the additional energy losses the beam undergoes in the upstream beamline will need to be evaluated in order to assess the impact of phase jitter measurement.

We can easily estimate the change in average fractional momentum from Reference [9]

$$\begin{aligned}\langle\delta\rangle_{CSR} &= -\frac{L_b}{\gamma_{ref}mc^2}\frac{2e^2N}{3^{1/3}(2\pi)^{1/2}R^{2/3}\sigma_z^{4/3}}\int_{-\infty}^{+\infty}dze^{-z^2/2\sigma_z^2}\int_{-\infty}^{z}\frac{d\xi}{(z-\xi)^{1/3}}\frac{d}{d\xi}e^{-\xi^2/2}, \\ &\simeq 0.350472\frac{r_eNL_b}{\gamma_{ref}R^{2/3}\sigma_z^{4/3}}, \end{aligned} \tag{9}$$

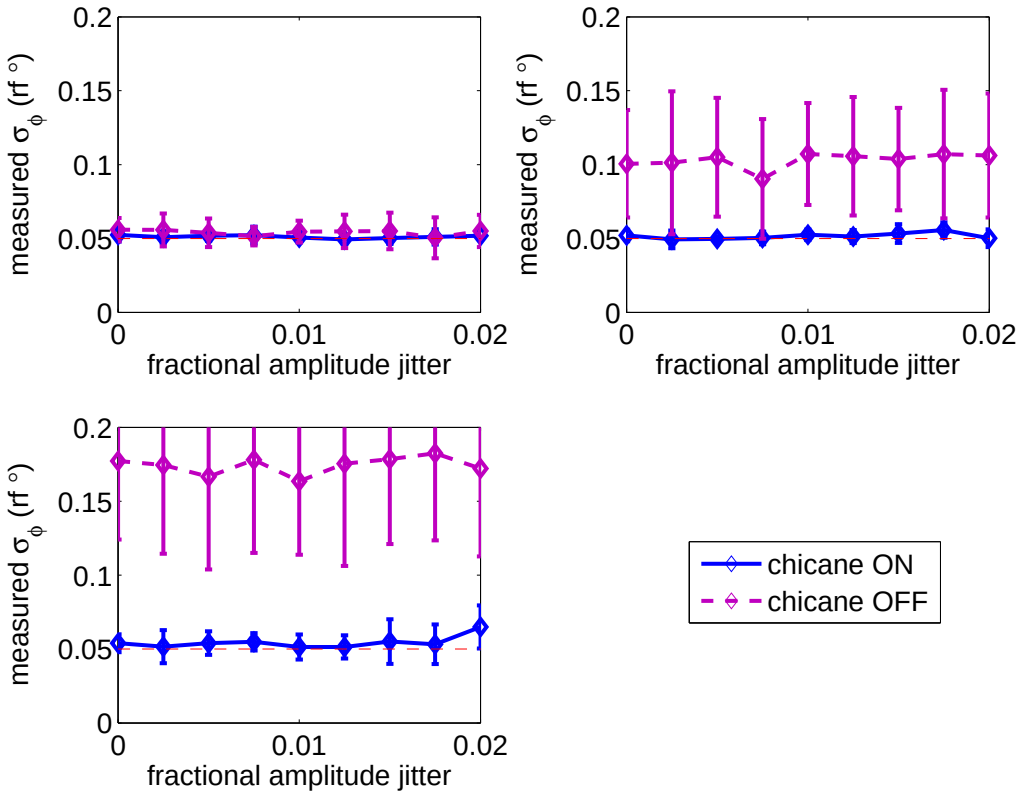

FIG. 5: Retrieved phase jitter as a function of the accelerating module's fraction amplitude jitter when the accelerating module phase is $\Phi = -50$ deg (top left), $\Phi = -10$ deg (top right) and $\Phi = -5$ deg (bottom).

where γ_{ref} is the reference energy, L_b the dipole length, R the radius of curvature of the trajectory, σ_z the rms bunch length, N the number of particle per bunch and r_e the classical radius of the electron. For our estimate we ignore transient CSR effects. Therefore a the bunch-to-bunch variation in energy loss will depend upon the bunch-to-bunch charge fluctuation. If the magnetic chicane is turned on such to measure the energy prior to the accelerating module only the CSR generated in the two last dipoles will need to be accounted for (both with $L_b = 20$ cm, $R = 0.6$ m, $\gamma_{ref} \simeq 80$). Similarly the energy loss induced in the spectrometer ($L_b = 1$ m, $R = 1$ m, $\gamma_{ref} \simeq 480$) downstream of the accelerator module will also bias the phase jitter measurement.

The other charge-dependent energy jitter source comes from wakefields. We assume the major source of wakefield to be induced in the accelerating module. Using reference [10], we find the fractional change in average energy due to the wakefield induced in one eight-cavities TESLA cryomodule to be

$$\langle \delta \rangle_{WKF} \simeq \frac{135Q}{\gamma_{ref} mc^2} \int_{-\infty}^{+\infty} dz \frac{1}{\sqrt{2\pi}\sigma_z} e^{-\frac{z^2}{2\sigma_z^2}} \int_{-\infty}^{z} ds 1.165 e^{-\sqrt{\frac{s-z}{3.65}}} - 0.165 e^{-\frac{s^2}{2\sigma_z^2}}, \qquad (10)$$

where Q has the units of pC in the latter equation The numerical values are obtained from a fit to time-domain simulations [10]. The energy loss is proportional to the charge per bunch, and the dependence on the rms bunch length is plotted in Fig. 6. For the nominal bunch parameters considered herein ($\sigma_z = 0.3$ mm, $Q = 3.2$ nC), the average energy loss is 0.36 MeV in the accelerating module. This corresponds to an average fractional momentum reduction of $\langle\delta\rangle \simeq 1.28\times10^{-3}$.

We gather in Table II the mean energy loss in the chicane and accelerating module. In order to insure the energy loss fluctuation is less than the resolution of the high energy spectrometer we need to insure that the bunch-to-bunch charge fluctuations to be $\langle(\Delta Q/Q)^2\rangle^{1/2} < 1$ % this would result in an rms relative total energy loss rms spread of 1×10^{-4}.

source	value
CSR half chicane	3.87×10^{-3}
CSR spectrometer	4.07×10^{-4}
wakefield in acc. module	1.28×10^{-3}
total loss	5.57×10^{-3}

TABLE II: Summary of coherent synchrotron radiation- and wakefield-induced energy loss downstream of the chicane's energy measurement station.

We now turn to specifying the charge fluctuation. In a photoinjector, the bunch charge depends on the photocathode drive laser intensity and on the electric field applied on the photocathode. The dependence on the electric field on the photocathode comes from the Schottky effect (tunneling effect). Considering Cesium Telluride photocathode the Schottky effect can be parametrized as $Q[nC] \propto Q_0(1 + 0.01)E_{cath}$ $[MV/m]$, where E_{cath} refers to the electric field (including both rf and space charge contributions) on the photocathode surface [11] and $Q_0 = 2.875$ nC was obtained from a series of calculations with Astra [12]. The field associated to the 1+1/2 cell ILCTA rf gun, along with the nominal photocathode drive laser settings (rms spot size on the photocathode of 1.4 mm and time profile consisting of four stacked Gaussian pulses with 2 ps duration each), were used as input in the Astra computer model. For changes in the electric field amplitude within $E \in [38, 40]$ MV/m, the relative variation of charge is found to be ~ 1.5 %. The total fraction rms

charge jitter is therefore given by

$$\langle(\Delta Q/Q)^2\rangle^{1/2} = \left[\langle(\Delta Q_0/Q_0)^2\rangle + \left(\frac{0.02}{E_{cath}^{-1}+0.02}\right)^2 \langle(\Delta E/E)^2\rangle\right]^{1/2}$$
$$\simeq \left[\langle(\Delta Q_0/Q_0)^2\rangle + 4.4\times10^{-3}\langle(\Delta E/E)^2\rangle\right]^{1/2}, \quad (11)$$

showing that the charge fluctuation is mainly dominated by laser intensity fluctuation: for pessimistic rms E-field relative amplitude jitter of ~ 5 % the contribution from E-field is of the order of 10^{-3}. Therefore the specified charge jitter essentially translates into laser intensity jitter: the rms laser intensity jitter should not exceed ~ 1 %.

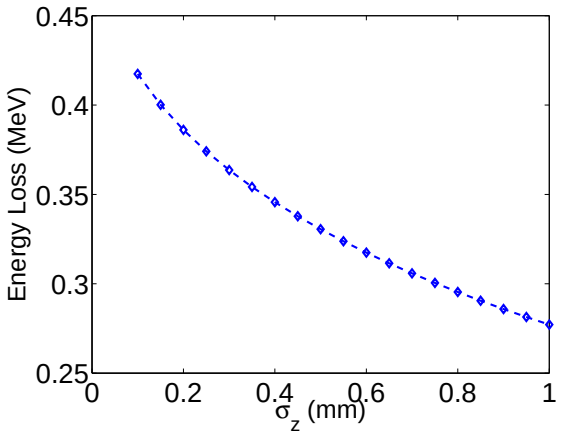

FIG. 6: Dependence of the wakefield-induced energy loss in a cryomodule (accounting only for geometric wakes induced by the shape of TESLA cavities) versus rms bunch length. The bunch is assumed to have a Gaussian longitudinal distribution and the charge per bunch is 3.2 nC.

B. Bunch-to-bunch pointing stability

Both monopole and dipole modes long range wakefields were also considered and found to result in negligible energy change – well below the resolution of our energy measurements. Finally another source of energy jitter coming from the radial dependence of the axial electric field in the TESLA cavity was investigated. From Maxwell's equation it can be shown that the off-axis expansion of the axial $E_z(z,r)$ field for a TM_{010}-mode cavity is given by

$$E_z(z,r) = \left[1 - \frac{r^2}{4}\left(1 - \partial_z^2 - \frac{\partial_t^2}{c^2}\right)\right] E_z(z, r=0), \quad (12)$$

where $E_z(z,0)$ is the axial electric field and r the considered radial offset. This effect was evaluated using ASTRA simulations and found to be insignificant (a particle with a 1 cm offset with respect to the cavity axis has its energy gain decreased by less than 1 keV compared to a particle accelerated on the cavity axis. Therefore there seems to be no specific requirement on the bunch-to-bunch pointing stability apart from those imposed by the single bunch beam dynamics.

VI. INSTRUMENTAL EFFECTS

In the previous Sections we did not address the consequences of instrumental errors on the time and energy measurements. We now consider these uncertainties in details and investigate the needed resolutions. State-of-the-art timing measurement are performed via electro-optical sampling techniques with sub-100 fs resolution [13, 14]. The energy measurement needs further analysis. Typically, and energy measurement consists of three beam position measurements: one measurement in a dispersive section and two others in an upstream (or downstream) dispersion-less region. The fractional energy offset, δ, with respect to the reference energy for which the dipoles in the dispersive section are set, is then given by

$$\langle\delta\rangle = \frac{\langle x\rangle - (R_{11}\langle x_0\rangle + R_{12}\langle x'_0\rangle)}{R_{16}}, \tag{13}$$

where the R are the transfer matrix element from a position upstream the dispersive section. The error on energy measurement is therefore:

$$\Delta\langle\delta\rangle = \frac{\Delta\langle x\rangle + |R_{11}\Delta\langle x_0\rangle| + |R_{12}\Delta\langle x'_0\rangle|}{|R_{16}|}, \tag{14}$$

If we consider a beam position monitor with resolution of 100 μm, we estimate the energy resolution to be of the order of 5×10^{-4} to 1×10^{-3}. In Figure 7 we consider the case of the accelerating module operated with $\Phi = -50$ deg and investigate the effects of resolution on the phase and energy measurements on the retrieved value for the phase jitter. Similar simulations for other cryomodule operating phase yield the same conclusion.

VII. SUMMARY

We performed an analysis of beam-based measurement of absolute phase jitter between an accelerating structure and a relativistic electron bunch. Our analysis included phase and energy

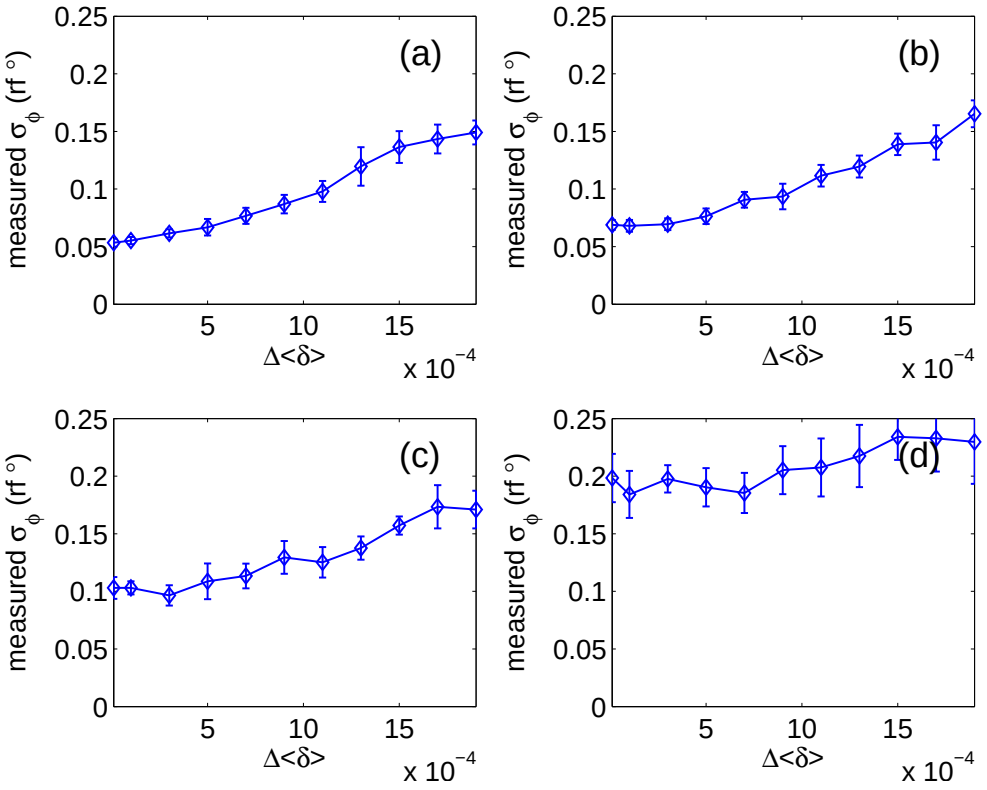

FIG. 7: Retrieved phase jitter as a function of uncertainty on the fractional energy measurement (both after and before the accelerating module) for four cased of resolution on time measurement of 50 (a), 100 (b), 200 (c) and 400 (d) femtosecond. For these simulations the accelerating module phase is set to $\Phi = -20$ deg. The energy resolution correspond to the chicane and the high energy spectrometer is assumed to have a lower resolution by a factor 3.

jitter upstream of the to-be-characterized accelerating module. Our conclusions are as follows. An energy measurement upstream of the accelerating module is needed in order to increase the resolution of the phase jitter measurement. The most straightforward energy measurement technique is to install a magnetic chicane (which can also serve other purposes). We also analyzed jitter coming from bunch-to-bunch charge fluctuations via collective effects (coherent synchrotron radiation and geometric wakefields for the example of a TESLA-type cryomodule) and found the bunch-to-bunch charge fluctuation should be maintained below 1 % (rms). Considering Schottky emission effect at the cathode we found that the requirement on bunch-to-bunch charge jitter directly translate into a requirement on the photocathode drive laser intensity which should be stabilized within 1 %. We however note that an alternative solution would be to monitor the charge of each bunch (using a beam current monitor; see Figure 1) and infer phase jitter values from a set of timing and energy

measurements within a defined bunch charge window.

---

[1] M. Church, ILC beamdocs, 1234 (2006)

[2] S. N. Simrock and T. Schilcher, "Transient beam loading based calibration of the vector sum for the Tesla Test Facility", Proceedings of the 1996 European Particle Accelerator (EPAC 96), Sitges Spain, 10-14 June 1996, pp. 1866-1868 (1996).

[3] K. Saito, "SCRF test facilities toward the ILC", in Proceedings of the 2006 European Particle Accelerator Conference (EPAC'06), Edinburgh UK, 26-30 June 2006, pp. 5-9 (2006).

[4] M. Church, S. Nagaitsev, and P. Piot, "Plans for a 750 MeV electron beam test facility at Fermilab", in Proceedings of the 2007 Particle Accelerator Conference (PAC'07), Albuquerque, New Mexico, 25-29 June 2007, pp 2942-2944 (2007).

[5] L. Wartski, *et al.*, *J. Appl. Phys.* **48**, 3646 (1975).

[6] K.-J. Kim, Nucl. *Instrum. Methods Phys. Res.*, Sect. **A 275**, 201 (1989).

[7] P. Piot, "A method to directly measure single bunch longitudinal wakepotentials", in preparation (2008).

[8] MATLAB is a registred software from The MathWorks, Inc.

[9] E. Saldin, E. A. Schneidmiller, and M. V. Yurkov, *Instrum. Methods Phys. Res.*, Sect. **A 398**, 373 (1997).

[10] A. Novokhatski, M. Timm and T. Weiland, "Single bunch energy spread in the TESLA cryomodule", TESLA-collaboration report TESLA 99-16 (1996).

[11] See G. Suberlucq, Proceedings of the 18th International free-electron laser conference (FEL 2006), Rome, 2006. Elsevier Science p. II-131. We started with the quantum efficiency parametrization (see Fig. 1, fit # 37) $\eta[\%] = 0.2 + 0.02E_{cath}[\mathrm{MV/m}]$ to assume a charge dependence of the form $Q = Q_0(1 + 0.1E_{cath}[\mathrm{MV/m}]$ and chose Q_0 to insure $Q(E_{rf} = 40) = 3.2$ nC. Note that the Reference does not discuss the importance of the space charge field in the reported measurement we assumed they were negligible – such an assumption is false in our case as illustrated by the devised value for Q_0 which was obtained from an iterative simulation with ASTRA.

[12] K. Flöttmann ASTRA *User Manual* DESY, 2002.

[13] A. L. Cavalieri, et al., *Phys. Rev. Lett* **94**, 114801 (2005).

[14] F. Loehl, et al., in *Proceedings of EPAC 2006* **94**, 114801 (2005).

[15] We assume the bunch length verifies $\sigma_z \ll \lambda_{rf}/(2\pi)$ where λ_{rf} is the wavelength associated to the radio-frequency system. If the assumption is not fulfilled then the energy gain takes the form $\gamma_k = \gamma_{0,k} + \Gamma_k \cos(\Phi_k) e^{-1/2\times(2\pi\sigma/\lambda_{rf})^2}$

Appendix: Description of the one-dimensional longitudinal dynamics model

A one dimensional model was developed to quickly estimate the impact of various sources of jitter on the longitudinal beam dynamics. The model is a MATLAB-based program. The implementation of each element is described in the following subsections. The program tracks a series of bunch represented by macroparticle in the longitudinal phase space (t, γ).

A. Photocathode drive-laser and rf-gun

Neglecting intensity fluctuations, the laser can only affect the longitudinal beam dynamics via its phase. The rf gun settings is described by two parameters: the E-field amplitude and phase between the laser and E-field. These two parameters set the initial conditions and the longitudinal motion is described by the system of coupled first order ordinary differential equations

$$\begin{aligned} \frac{d\psi}{dz} &= k\left(\frac{\gamma}{\sqrt{\gamma^2-1}}-1\right), \\ \frac{d\gamma}{dz} &= 2\alpha k\hat{E}_z \sin(\psi + kz), \end{aligned}$$

where $\alpha \equiv \frac{eE_0}{2kmc^2}$ is the normalized accelerating field [6], E_0 is the peak E-field, $k \equiv \frac{2\pi}{\lambda}$ and $\hat{E}_z(z)$ is the normalized on-axis E-field obtained from, e.g., SUPERFISH simulations. There is generally no closed-form solution of such a system, and the equations of motion are generally numerically integrated. In [6] an approximate solution is derived using the method of successive approximation and a bunch compression factor is inferred but this leads to large error on the time calculation and to non physical values of the analytically computed compression factor. Therefore we chose to numerically integrate the longitudinal motion using a fourth order Runge-Kutta. Am example of such numerical integration showing the sensitivity, at the gun exit, of the time of flight and energy of a bunch as a function of the gun amplitude and laser launch phase is presented in Fig. 8.

B. Drift spaces

In the absence of radiation process, the bunch total energy remains constant in a drift. The time-of-flight of the bunch depends on the bunch energy via $t = \frac{L}{v} = \frac{L}{c}\left[1-\frac{1}{\gamma^2}\right]^{-1/2}$. The transformation

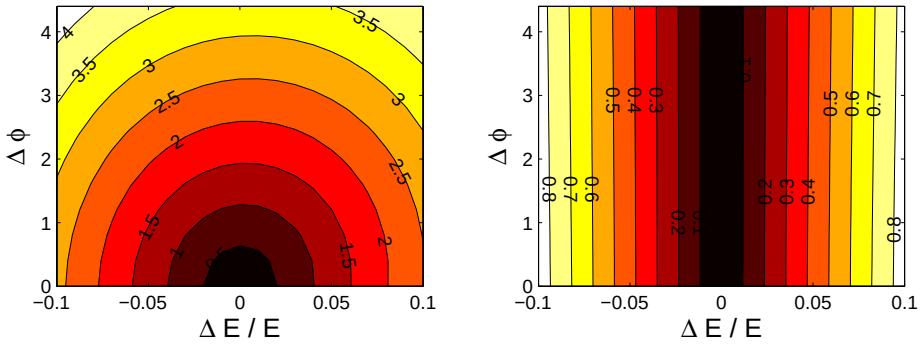

FIG. 8: Sensitivities of the phase (left) and γ Lorentz factor (right) at the rf-gun exit as a function of the laser launch phase ϕ and rf-gun E-field relative amplitude jitter $\Delta E/E$. The phase jitter unit is degree and the Lorentz factor is dimensionless.

through a drift is therefore

$$\begin{aligned} t_f &= t_0 + \frac{L}{c}\left(1 + \frac{1}{2\gamma^2}\right), \\ \gamma_f &= \gamma_0. \end{aligned}$$

For electrons this is a noticeable effect only at low energy (e.g. in the drift from the rf gun to the cavity entrance). At low energy the drift can map an energy jitter into a time jitter.

C. Accelerating cavities

A cavity changes both the beam energy and can introduce an energy dependent time-of-flight. Given a bunch initial longitudinal coordinates (t_0, γ_0), the final coordinate are:

$$\begin{aligned} t_t &= t_0 + \frac{L_{acc}}{c}\left(1 + \frac{1}{2}\frac{1}{\gamma_0\gamma_f}\right) \\ \gamma_f &= \gamma_0 + \Gamma\cos(\omega t_0 + \Phi), \end{aligned}$$

where Γ and Φ are the operating voltage and phase of the accelerating section, and L_{acc} the effective length of the accelerating structure.

D. bunch compressor chicane

The chicane consists of four dipole magnets; see Fig. 9. The energy of a bunch is unaffected (ignoring synchrotron radiation), and the time-of-flight can be deduced from simple geometric arguments: the path length is given by $L = 4L_B\frac{\theta}{\sin\theta} + L_i + 2\frac{L_0}{\cos\theta}$ where θ is a function of γ. The

coordinate of a bunch are mapped accordingly to

$$\begin{aligned} t_f &= t_0 + \frac{1}{c}\left(4L_B\frac{\theta}{\sin\theta} + L_i + 2\frac{L_0}{\cos\theta}\right) \\ \gamma_f &= \gamma_0, \end{aligned}$$

where $\theta = \arcsin\left(\frac{\gamma_{nom}}{\gamma}\sin\theta_{nom}\right)$ with θ_{nom} corresponding to the nominal bending angle for the nominal bunch energy.

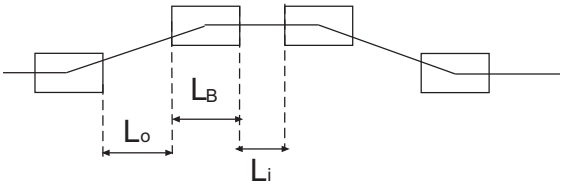

FIG. 9: Bunch compressor chicane model used in the simulations.